PNAS RESEARCH ARTICLE | ECOLOGY SUSTAINABILITY SCIENCE OPEN ACCESS

Global collision-risk hotspots of marine traffic and the world's largest fish, the whale shark

Freya C. Womersley[a,b,1], Nicolas E. Humphries[a], Nuno Queiroz[a,c], Marisa Vedor[c], Ivo da Costa[c], Miguel Furtado[c], John P. Tyminski[d], Katya Abrantes[e,f,g], Gonzalo Araujo[h,i], Steffen S. Bach[j], Adam Barnett[e,f,g], Michael L. Berumen[k], Sandra Bessudo Lion[l], Camrin D. Braun[m,n], Elizabeth Clingham[o], Jesse E. M. Cochran[k], Rafael de la Parra[p], Stella Diamant[q], Alistair D. M. Dove[r], Christine L. Dudgeon[s], Mark V. Erdmann[t], Eduardo Espinoza[u,v], Richard Fitzpatrick[e,f], Jaime González Cano[w], Jonathan R. Green[x], Hector M. Guzman[y], Royale Hardenstine[k], Abdi Hasan[z], Fábio H. V. Hazin[aa], Alex R. Hearn[v,bb], Robert E. Hueter[d,cc], Mohammed Y. Jaidah[dd], Jessica Labaja[h], Felipe Ladino[l], Bruno C. L. Macena[aa,ee], John J. Morris Jr.[d], Bradley M. Norman[ff,gg], Cesar Peñaherrera-Palma[v], Simon J. Pierce[hh], Lina M. Quintero[l], Dení Ramírez-Macías[ii], Samantha D. Reynolds[gg,jj], Anthony J. Richardson[kk,ll], David P. Robinson[mm], Christoph A. Rohner[hh], David R. L. Rowat[nn], Marcus Sheaves[e,g], Mahmood S. Shivji[oo], Abraham B. Sianipar[pp], Gregory B. Skomal[qq], German Soler[l], Ismail Syakurachman[pp], Simon R. Thorrold[n], D. Harry Webb[r], Bradley M. Wetherbee[oo,rr], Timothy D. White[ss], Tyler Clavelle[ss], David A. Kroodsma[ss], Michele Thums[tt], Luciana C. Ferreira[tt], Mark G. Meekan[tt], Lucy M. Arrowsmith[uu], Emily K. Lester[uu], Megan M. Meyers[uu], Lauren R. Peel[vv], Ana M. M. Sequeira[vv], Victor M. Eguíluz[ww], Carlos M. Duarte[k], and David W. Sims[a,b,xx,1]

Edited by Peter Kareiva, University of California, Los Angeles, CA; received October 6, 2021; accepted February 26, 2022

Marine traffic is increasing globally yet collisions with endangered megafauna such as whales, sea turtles, and planktivorous sharks go largely undetected or unreported. Collisions leading to mortality can have population-level consequences for endangered species. Hence, identifying simultaneous space use of megafauna and shipping throughout ranges may reveal as-yet-unknown spatial targets requiring conservation. However, global studies tracking megafauna and shipping occurrences are lacking. Here we combine satellite-tracked movements of the whale shark, *Rhincodon typus*, and vessel activity to show that 92% of sharks' horizontal space use and nearly 50% of vertical space use overlap with persistent large vessel (>300 gross tons) traffic. Collision-risk estimates correlated with reported whale shark mortality from ship strikes, indicating higher mortality in areas with greatest overlap. Hotspots of potential collision risk were evident in all major oceans, predominantly from overlap with cargo and tanker vessels, and were concentrated in gulf regions, where dense traffic co-occurred with seasonal shark movements. Nearly a third of whale shark hotspots overlapped with the highest collision-risk areas, with the last known locations of tracked sharks coinciding with busier shipping routes more often than expected. Depth-recording tags provided evidence for sinking, likely dead, whale sharks, suggesting substantial "cryptic" lethal ship strikes are possible, which could explain why whale shark population declines continue despite international protection and low fishing-induced mortality. Mitigation measures to reduce ship-strike risk should be considered to conserve this species and other ocean giants that are likely experiencing similar impacts from growing global vessel traffic.

ship strike | marine megafauna | conservation | movement ecology | human impact

Significance

Global vessel traffic is increasing alongside world economic growth. The potential for rising lethal ship strikes on endangered species of marine megafauna, such as the plankton-feeding whale shark, remains poorly understood since areas of highest overlap are seldom determined across an entire species range. Here we show how satellite tracking whale sharks and large vessel movements globally provides a means to localize high-overlap areas and to determine how collision risk changes in time. Our results point to potential high levels of undetected or unreported ship strikes, which may explain why whale shark populations continue to decline despite protection and low fishing-induced mortality. Collision mitigations in high-collision-risk areas appear necessary to help conserve this iconic species.

Global trade relies on maritime transport, with >80% of merchandise by volume carried by sea (1). The world's merchant fleet has risen from 1,771 vessels >100 gross tons to more than 94,000 in the last 25 y (1995 to 2020) (1, 2). Maritime transport is expected to increase alongside world economic growth (1), presenting a growing threat to a large number of marine megafauna species such as cetaceans, sea turtles, and fish (3, 4). Threats to wildlife from expanding maritime activities include direct exploitation (5, 6), close-range interactions (4, 7), and associated stressors such as anthropogenic noise pollution (8) and entanglement in fishing gear (9). In particular, collisions with large, relatively fast-moving vessels can result in direct mortality of wildlife (10). For endangered marine megafauna with low population sizes that are slow-moving and occupy surface waters in heavily trafficked areas, fatal collisions may be the primary factor preventing population recovery (11). Marine mammal collisions with ships have received considerable research attention for several decades (4, 7), leading to ship strikes being identified as a priority conservation concern by the International Whaling Commission in 2005 (12). However, information on fatal collisions from ship strikes is usually only available in limited parts of a species' distributional range, hence range-wide population effects on many surface-dwelling megafauna (including large, plankton-feeding fish) remain poorly understood.

The whale shark, *Rhincodon typus*, is a planktivorous elasmobranch reaching lengths up to 18 to 20 m (13, 14) that is listed as "endangered" by the International Union for

The authors declare no competing interest.

This article is a PNAS Direct Submission.

[1]To whom correspondence may be addressed. Email: f.womersley@mba.ac.uk or dws@mba.ac.uk.

This article contains supporting information online at http://www.pnas.org/lookup/suppl/doi:10.1073/pnas.2117440119/-/DCSupplemental.

Published May 9, 2022.

the Conservation of Nature (IUCN) Red List (15). Although international trade in whale shark meat, fins, and other products has been regulated by the Convention on International Trade in Endangered Species (CITES) since 2003, the cause of continued decline in whale shark numbers at several locations worldwide is unclear and cannot be explained by fishing or other related impacts alone (15, 16). Recent studies have recorded injuries and healed scars on surviving whale sharks resulting from interactions with smaller coastal vessels (e.g., speed boats) which are unlikely to cause direct mortality from a collision (4, 17). However, since whale sharks are distributed worldwide [in tropical, subtropical, and warm temperate seas (18)], spend significant amounts of time in surface waters (14), and aggregate seasonally in specific areas where heavy shipping traffic appears common (19–21), there is concern that collision with larger vessels may be a substantial source of unrecorded "cryptic" mortality that may drive observed population declines (15).

A major challenge to understanding global marine megafauna mortalities from collisions with large vessels is the lack of direct observations. Whale sharks, for example, sink when dead, and thus the vast majority of mortalities likely go unnoticed (*SI Appendix*, sections 4.1 and 4.2). Given the need to identify where hidden mortality may be occurring, estimating collision risks from fine to ocean-wide scales based on dynamic patterns of ship density and animal distributions are required. Previous studies estimating collision risk at large, regional scales lack animal occurrence data across the majority of the area studied and therefore relate ship densities to the probability of animal occurrence or predicted density calculated from habitat suitability models (for review see ref. 4). These approaches provide only general estimates of collision risk since predicted suitable habitat or density alone cannot explicitly account for the highly heterogeneous patterns of individual animal movements. The collision risk for aggregations and areas of prolonged residency of marine megafauna in heavily trafficked areas, or from repeated movements across the busiest shipping lanes for example, may be underestimated by these approaches (22). Global assessments of the impacts of vessel traffic on marine megafauna have yet to use individual animal and ship movement data across entire species distributions to provide global-scale synoptic estimates of spatiotemporal collision risks (4). The combination of large animal and vessel tracking datasets (5, 23) could underpin systemic, global assessments that are independent of collision-risk estimates based on anecdotal reports of vessel-related injuries observed on surviving animals or coarse-resolution modeled occurrence.

Here, we provide global estimates of potential fatal collision risk of marine traffic composed of large vessels (defined here as >300 gross tons) with an ocean giant, the whale shark, which may serve as a model approach for other marine megafauna. Satellite tracks of individual whale sharks were collated through the Global Shark Movement Project (GSMP, https://www.globalsharkmovement.org), a worldwide research collaboration of over 150 shark scientists using telemetry/bio-logging techniques to map threatened shark space-use patterns ocean-wide in relation to changing environments and anthropogenic threats (5). The current study on whale sharks was formed in 2019 as a GSMP subproject involving 69 scientists from 23 research groups in 44 institutes across 18 countries (*SI Appendix*, sections 6–8). Positions from satellite-tracked whale sharks and vessel movements from Automatic Identification System (AIS) data were analyzed across the whale sharks' global range to estimate spatiotemporal overlap and the susceptibility of sharks to collisions with large commercial vessels across major ocean regions (*Methods* and *SI Appendix*, Table S1 and Fig. S1). We focused on large vessels because global data are available and such vessels have been recorded more often in fatal collisions with whale sharks compared to interactions with smaller vessels (primarily in coastal areas) that are more likely to lead to survivable injuries (4, 10) (*SI Appendix*, section 4.7). Our approach of using dynamic, satellite-tracked movements of sharks and vessels to identify fine-scale (tens of kilometers), spatially explicit collision-risk areas enables targeted mitigation measures. Additionally, depth-recording pop-off satellite tags attached to sharks relay depth data directly to satellites when they float back to the surface after release, potentially recording the sinking of a dead shark following a ship-strike mortality event.

Results and Discussion

Whale Shark Movements. Tracks from 348 individual whale sharks, tagged in all of the main ocean regions where they are found (*SI Appendix*, Table S2), demonstrated that individuals regularly exhibit area-restricted local movements interspersed by long-distance travel (Fig. 1*A*). Tracking data (Fig. 1*A*) confirmed known aggregation areas, including the northern coast of West Papua, the northwestern coast of Australia, the Pacific coast of Panama, Qatari waters in the Arabian Gulf, and the northeastern coast of the Yucatán Peninsula, Mexico (*SI Appendix*, Figs. S2*B* and S3*A*). Tracked whale sharks often made long-distance movements from coastal areas into oceanic waters before returning to aggregation sites (Fig. 1*A*). For example, several sharks in the west Pacific moved from coastal West Papua (Indonesia) into oceanic waters before returning each season over several years, indicating a fidelity to persistent aggregation sites within annual movement patterns. Males, which accounted for at least 47.4% of satellite tags deployed globally, spent more time in coastal waters (52.7% locations ≤200 m depth) than females (22.2% locations ≤200 m) (Fig. 1*A*). Using depth-recording tags we found whale sharks spent almost half of their total tracked time (median 45.7%, $n = 39{,}143$ depth records; *SI Appendix*, Table S3) in surface waters (≤20 m, or ≤25 m for the east Pacific) that coincided vertically with the draft depths and associated hydrodynamic draw of moving large-ship hulls (24) (Fig. 1*B*) (*Methods* and *SI Appendix*). Satellite tracks and depth data confirmed the potential exposure of individual whale sharks to large vessels in both coastal and oceanic areas (Fig. 1 *A* and *B* and *SI Appendix*, section 4).

The global map of whale shark relative density (Fig. 2*A*) from tracked individuals revealed space-use hotspots (defined here as ≥90th percentile of the mean weighted daily location estimates within each cell, which are displayed as volume contours in *SI Appendix*, Fig. S3*A* and see *Methods*). Space-use hotspots were evident in the Atlantic Ocean (Gulf of Mexico, St. Helena), Indian Ocean (Arabian Gulf, the Red Sea, northwest Madagascar, western Australia), and the Pacific Ocean (Gulf of California, Gulf of Panama, Panama Basin, New Guinea, the Philippines) (Fig. 2*A* and *SI Appendix*, Fig. S3*A*). Hotspots were characterized by individuals remaining resident, or returning there posttagging, relative to adjacent areas where space use was lower. Although tagging sites can bias the identification of space-use hotspots, we reduced this effect by employing a track-length weighting procedure (see *Methods*) (5). Using this approach, we also identified whale shark space-use hotspots where no tagging took place, for example in the north Atlantic (Texas-Louisiana shelf, Mexico Basin, Bay of Campeche), east Indian Ocean (region extending off Perth Canyon shelf edge), west Pacific (Timor Sea, Ceram Sea, Arafura Sea, Caroline and Makur Islands), and the east Pacific (where the Equatorial

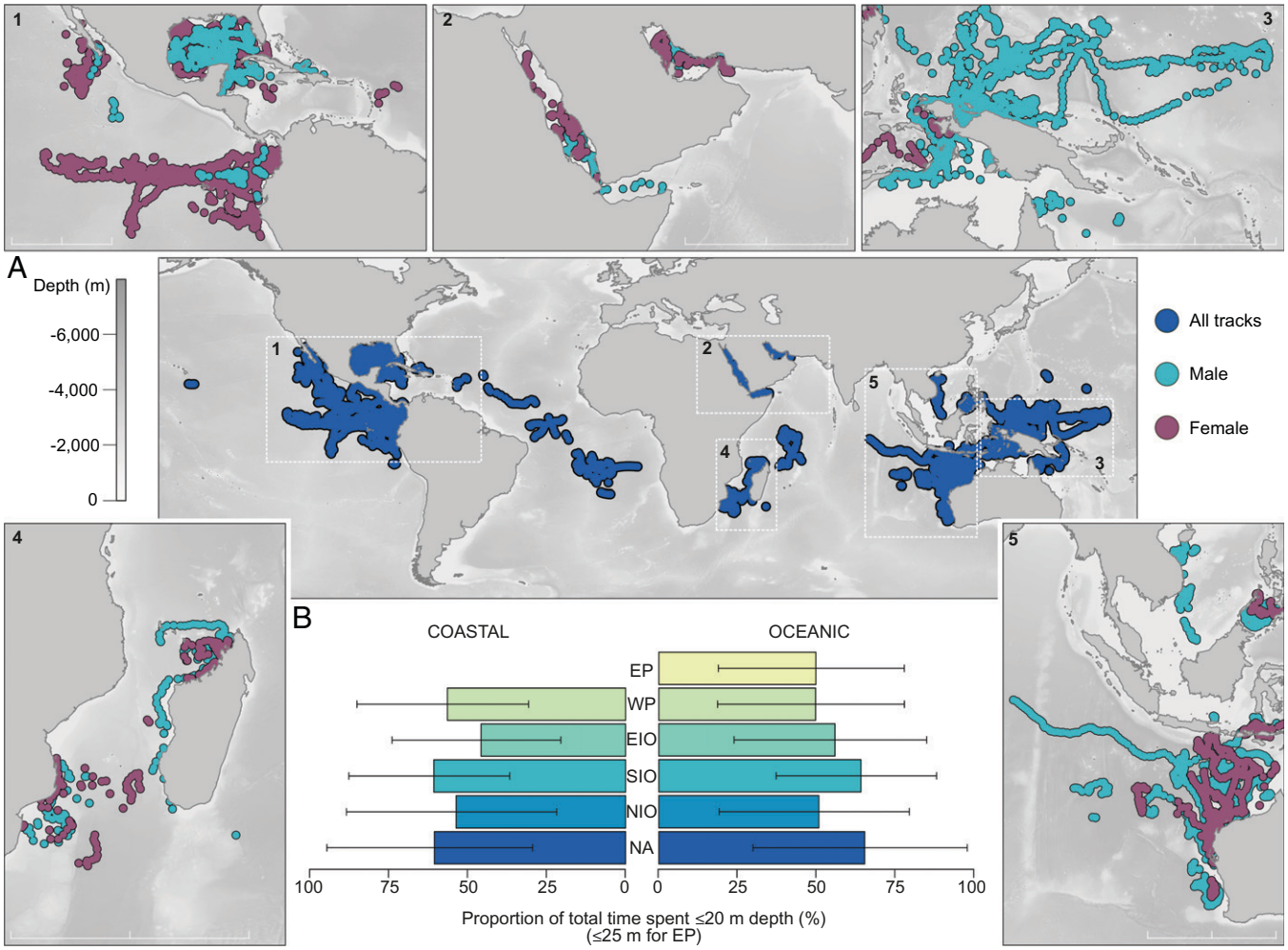

Fig. 1. Global whale shark horizontal and vertical movements. (*A*) Estimated whale shark positions for 348 individual tracks obtained via satellite transmitters deployed from 2005 to 2019 with sex differences given in the panels. (*B*) Mean proportion of total time (percent) spent shallower than 20-m depth (collision-risk zone) (shallower than 25-m depth for the east Pacific region) in each region from depth-sensitive tag records associated with coastal (≤200-m depth) and oceanic (>200-m depth) habitats. Error bars denote ± one SD of the mean. EP, east Pacific; WP, west Pacific; EIO, east Indian Ocean; SIO, southwest Indian Ocean; NIO, northwest Indian Ocean; NA, north Atlantic; SA, south Atlantic. (Scale bars: 1,000 km.)

Counter Current diverges northward, shelf edge off Ecuador and Peru, Cocos Ridge) (*SI Appendix*, Figs. S2*A* and S3*A*).

Marine Traffic Patterns. Movements of vessels equipped with AIS receivers (>300 gross tons, as required by the International Maritime Organization, IMO) were mapped on a mean monthly basis (2011 to 2014 and 2017 to 2019) to estimate the extent of space-use overlap of whale sharks and vessels (Fig. 2*B*). Maps of global vessel-traffic density revealed several trans-oceanic shipping routes (characterized as ≥90th percentile of unique vessel counts within 0.25 × 0.25° (~28 km of latitude) grid cells; 31 vessels for 2011 to 2014 annual mean), connecting, for example, Cape Town to Singapore and Singapore to Dubai and through the Suez Canal to Port Said (Fig. 2*B* and *SI Appendix*, Fig. S4). Similarly, there were several areas heavily used by vessels outside explicit shipping routes (defined as ≥75th percentile of unique vessel counts within grid cells; 10 vessels for 2011 to 2014 annual mean), including the Gulf of Mexico, Caribbean Sea, Arabian Gulf, Arabian Sea, and the South China Sea. These areas were mostly used by cargo and tanker vessels that showed little spatial variation over monthly timescales but generally had a greater maximum vessel count in the latter half of the year (July to December; *SI Appendix*, Fig. S4). There were few areas where vessel traffic density appeared sparse and these were generally outside the whale sharks' distribution (poleward of 55°S and 75°N). Overall, we found low temporal variation in vessel density within the geographical range of whale sharks (Fig. 2*C*), indicating the busiest shipping routes were temporally consistent, including in areas where they overlapped with individuals in the dataset.

Shark–Vessel Interactions. Close-range interactions between whale sharks and vessels underpin our estimates of broader-scale overlap and potential collision risk. At the regional scale, there was monthly variation in spatial density of whale sharks (Fig. 3*A* and *SI Appendix*, Fig. S5), where individuals aggregated seasonally on finer geographic scales before undertaking larger-scale movements often into oceanic areas (Fig. 3*A*). Analysis of selected individual tracks per region showed that, during their annual movements, whale sharks moving away from aggregations routinely crossed busy shipping routes where potential for interactions is higher (Fig. 3 *B* and *C* and *SI Appendix*, Fig. S6). For example, a west Pacific whale shark crossed a shipping route in July/August where the maximum monthly vessel count in occupied grid cells was >100 vessels (2011 to 2014 annual mean), before moving into the deep Pacific for several months, only to return and transit the same shipping route in January/February when the maximum

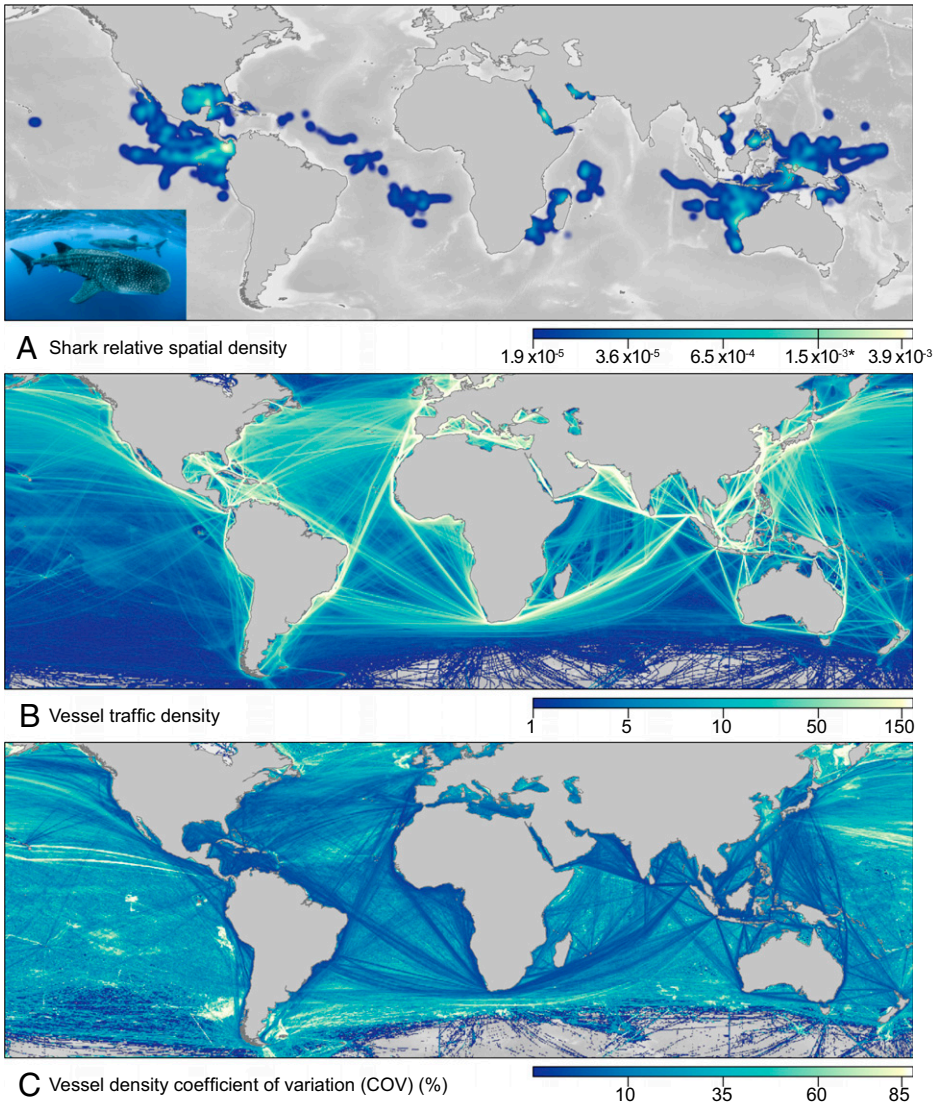

Fig. 2. Spatial distribution of whale sharks and global vessel movements. (*A*) Relative density of whale sharks. Kernel distribution of the mean monthly sum of weighted and normalized location estimates of tracked whale sharks within each 0.25° × 0.25° resolution cell (hotspots of occupancy were defined as ≥90th percentile of mean relative density with a 2.5° radius applied). Lighter colors reflect higher densities of sharks. (*Inset*) Image of multiple whale sharks; credit: S.J.P. (*B*) Vessel traffic density (total count of vessels within 0.25° × 0.25° resolution cells). Mean annual total number of AIS-tracked vessels averaged for the years 2011 to 2014 (see *Methods*). Lighter colors reflect higher densities of vessels. (*C*) Coefficient of variation (percent) for vessel traffic density displaying annual variation at a 0.25° × 0.25° cell resolution scale. Darker colors denote lower variation.

monthly density had increased to >250 vessels (Fig. 3*B*). A similar pattern was also evident in the east Pacific, where a whale shark crossed the same shipping route in both January and September during a southward movement, encountering monthly vessel densities of ∼150 and ∼300 vessels, respectively (Fig. 3*C*). Within ocean regions, there were zones of higher space use of sharks during transit, used by multiple individuals that overlapped routes of dense large-vessel traffic (*SI Appendix*, Fig. S7 and see *Methods*). For instance, movement extents of whale sharks tracked in the Red Sea and Arabian Sea were almost entirely overlapped by shipping routes (*SI Appendix*, Fig. S7*B*). Moreover, fine-scale analysis of two Global Positioning System (GPS)-tagged whale sharks (<170 m location accuracy) in relation to large vessels' routes within the Gulf of Mexico (Fig. 3 *D* and *E* and *SI Appendix*, Fig. S8) demonstrated that vessels routinely passed very close to the tagged whale sharks at speeds averaging over 10 times faster than those of sharks (mean closest point-of-approach ship speeds = 3.84 $m{\cdot}s^{-1}$ ± 2.19 SD; mean estimated shark speeds = 0.31 $m{\cdot}s^{-1}$ ± 1.83 SD) (Fig. 3 *D* and *E* and *SI Appendix*, Fig. S8 and Table S4), and with vessels having a maximum draft of 14.5 m, which extends from the surface into more than 70% of the collision zone use depth limit of ≤20 m applied in this study (see *Methods*). On average, a large vessel crossed the 2,130 km and 1,852-km-long shark GPS tracks every 3.1 and 12.0 km, respectively (Fig. 3 *D* and *E* and *SI Appendix*, Fig. S8 and Table S4), indicating the potential for recurrent shark–vessel interactions given the frequent proximity of large vessels to whale shark aggregations, high-residency sites, and long-range coastal and oceanic seasonal shark movements. Furthermore, observational anecdotes and formalized research dating back to the 1820s suggest that whale sharks show limited horizontal or vertical avoidance behaviors in the presence of vessels moving at normal operational speeds, even those approaching at close range (*SI Appendix*, Table S5), which further highlights the potential for fatal collisions to occur in the aforementioned circumstances.

Spatiotemporal Overlap. The spatial overlap of tracked whale sharks with global vessel activity, defined as the co-occurrence of sharks and vessels within the same 0.25 × 0.25° grid cell in an average month, was calculated for each shark within the

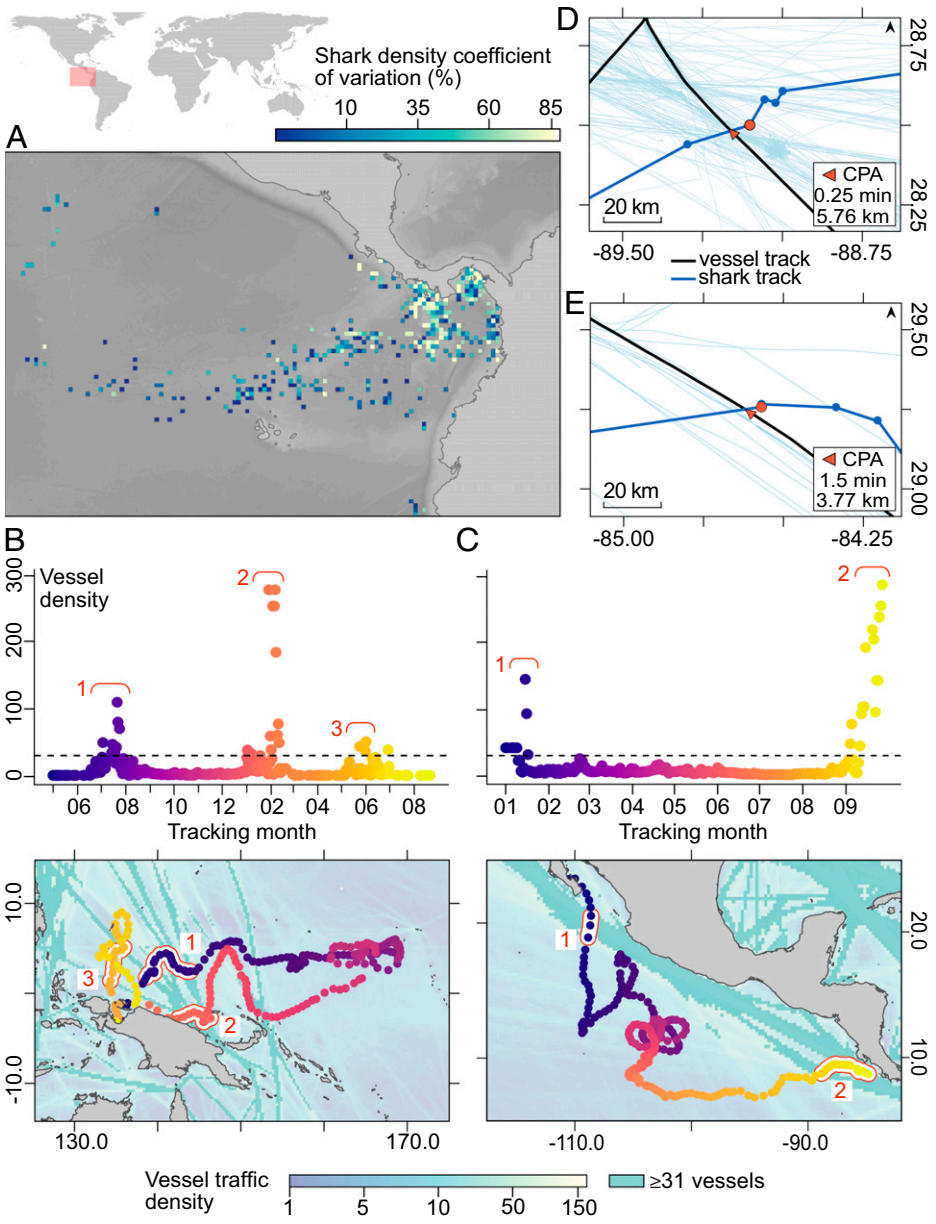

Fig. 3. Individual whale shark movements. (*A*) Coefficient of variation (percent) for shark density displaying annual variation at a 0.25° × 0.25° cell resolution within an example area of the east Pacific region. Darker colors denote lower variation. (*B* and *C*) Individual shark movements around busy vessel routes. Examples of two whale sharks that moved out from and back to known aggregation areas compared to the number of vessels encountered at each tracked location (*y* axis, 2011 to 2014 annual mean) through time. Locations where individuals move through cells with busy traffic (defined as the top 90th percentile of vessel counts within a cell; 31 for the 2011 to 2014 annual mean, displayed as black dotted line in upper panels) are highlighted and numbered when (*Upper*) and where (*Lower*) the sharks pass through these areas during tracked movements. Cells with vessel counts representing busy routes have been colored uniformly in maps to aid interpretation. (*D* and *E*) Fine-scale shark–vessel interactions. Examples of simultaneous vessel and whale shark tracking in the Gulf of Mexico in the year 2018 displaying the closest point of approach (CPA) time difference and distance from two close encounters within the dataset.

dataset (see *Methods*). The detailed analysis of whale shark overlap with vessels focused on combined vessel types to establish potential risk from all tracked vessels >300 gross tons. Globally, the distribution of vessel activity in the dataset overlapped 92.4% of the mean monthly space used by tracked whale sharks (±14.1 SD monthly overlap; median 100%, $n = 348$ tracks). Across the seven distinct regions, mean monthly spatial overlap values ranged from 86.6 to 100.0% (Fig. 4 *A* and *B* and *SI Appendix*, Table S6*A*).

Global space use by whale sharks overlapped more with cargo vessels than any other vessel class (mean monthly overlap, 82.3%), and least with fishing vessels (34.7%) (Fig. 4*C* and *SI Appendix*, Table S7). Individuals occupying the north and south Atlantic regions experienced the highest overlap with cargo vessels (mean monthly overlap in north Atlantic, 97.4%, $n = 39$ tracks; south Atlantic, 99.9%, $n = 14$ tracks), and north Atlantic sharks were also exposed to high overlap with passenger (72%, $n = 39$ tracks) and tanker vessels (92.8%, $n = 39$ tracks) (*SI Appendix*, Table S7). Individuals occupying the east Pacific experienced the highest overlap with fishing vessels (49.3%, $n = 89$ tracks), with spatial overlap of sharks and fishing vessels over 40% higher than in the west Pacific region (8.4%, $n = 62$ tracks) (*SI Appendix*, Table S7). Although values of mean monthly overlap remained high (>85%) across regions (Fig. 4*B* and *SI Appendix*, Table S6), indicating high spatial persistence in exposure of sharks to vessels across the global

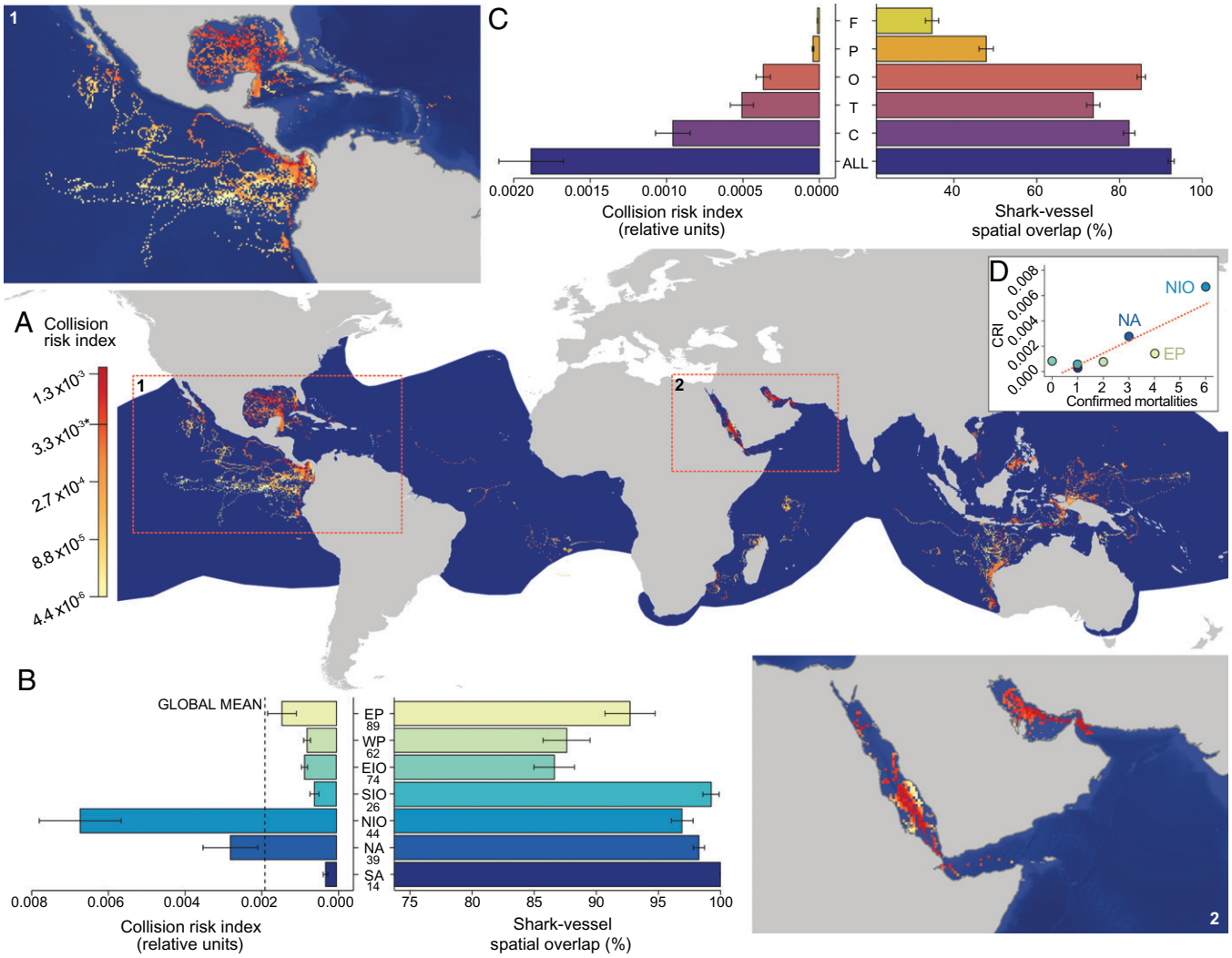

Fig. 4. Spatial distribution of overlap and risk. (*A*) Map showing distribution of the mean monthly overlap and CRI that whale sharks were exposed to in overlapping areas within each 0.25° × 0.25° resolution cell. Hotspots of collision risk were defined as cells with ≥90th percentile of mean relative CRI. Red cells represent higher relative CRI than yellow cells. The current whale shark distribution taken from the IUCN is shown as the dark blue shaded area. (*B*) Mean monthly CRI (*Left*) and overlap (*Right*) experienced by individuals within each region (error bars denote ± one SEM) with global mean displayed as dotted line. EP, east Pacific; WP, west Pacific; EIO, east Indian Ocean; SIO, southwest Indian Ocean; NIO, northwest Indian Ocean; NA, north Atlantic; SA, south Atlantic. Number below each region abbreviation is the number of shark tracks for that region. (*C*) Mean monthly CRI (*Left*) and overlap (*Right*) experienced by individuals from a range of vessel types (error bars denote ± SE). F, fishing; P, passenger; O, other; T, tanker; C, cargo. (*D*) Mean monthly CRI correlated with total number of confirmed large-vessel-related mortalities recorded from each region (*SI Appendix*, Table S8). Dotted line shows best fit from linear regression.

ocean (Fig. 2*C*), there was distinct temporal variation in spatial overlap between whale sharks and vessels (*SI Appendix*, Fig. S9) that reflects movements of sharks (Fig. 3).

Global Collision-Risk Estimates. To estimate potential exposure of whale sharks to large vessels and the subsequent potential risk of collision, we calculated a mean monthly collision-risk index (CRI) for each individual shark (*Methods*, Fig. 4*A*, and *SI Appendix*, Fig. S1). We calculated CRI as the product of potential collision exposure (E_i, which adjusts for regional collision zone use, z_i) and shark spatial density (D_{it}, standardized to account for variations in durations of individual tracks) (see *Methods*). Given the close proximity of vessels and shark positions highlighted by fine-scale simultaneous tracking (Fig. 3 and *SI Appendix*, Fig. S8 and Table S4), we assumed that whale sharks with both a high overlap with vessel activity and a high CRI would be at greater potential risk of collision than those with a lower overlap and CRI (*SI Appendix*, Fig. S10). However, the probability of a collision within regions will depend on several factors related to both whale shark behaviors and vessel characteristics. Because shark horizontal swimming speeds were 10 times slower than vessel speeds (*SI Appendix*, Table S4), whale sharks may be much less able to avoid an oncoming vessel, particularly since if they do exhibit a response it appears slow and limited to until vessels are very close (*SI Appendix*, Table S5) (25). We were able to determine from tags with depth sensors the proportion of time whale sharks spent near the surface, where they were most at risk of collision (collision zone use, z_i). However, at the global scale we could not record avoidance responses of sharks to vessels (*SI Appendix*, Table S5) (25), characterize the type of behavior when at the surface (26), or the range at which oncoming vessels were detected (27, 28). Similarly, vessel maneuverability, speed (29), and overall size and draft (24) will also contribute to the risk of collision. To date there are few studies that explore fine-scale behaviors in sufficient detail to include behavioral aspects into collision-probability estimates for whale sharks (25, 30). Given this, our CRI provides an estimate of the risk of collision with large vessels within an area based on the degree of spatiotemporal co-occurrence (hence susceptibility), rather than providing a

probability estimate of an actual ship strike (vulnerability) (*SI Appendix*, section 4.2).

Validation of CRI as a relative measure of whale shark mortality risk from large vessels is challenging because reporting of whale shark collisions with large vessels is not mandated by the IMO, and a global database of fatal collisions has yet to be assembled. However, as a first step, we collated fatal collision reports from the published literature and media reports where location and mortality were confirmed (*SI Appendix*, Table S8). Regional mean monthly CRI correlated positively with reported whale shark mortality (Pearson's $r = 0.86$, $n = 7$ regions, $P = 0.013$; *SI Appendix*, Table S8) and 50% ($n = 16$ incidences) of reported mortalities' locations fell within the 75th percentile contour of CRI, suggesting that regions with high CRI are also likely to have higher mortality of whale sharks due to collisions with large vessels (Fig. 4*D* and *SI Appendix*, Fig. S3*B*). Further, CRI estimates were not correlated with percentage occurrence of vessel-related injuries on a local scale (Pearson's $r = -0.03$, $n = 10$ regions, $P = 0.99$) (*SI Appendix*, section 4.7 and Table S9), suggesting these nonfatal injuries were likely inflicted mainly in coastal areas by smaller vessels not using AIS, an explanation supported by previous studies (4) (see also references in *SI Appendix*, Table S9).

Across the seven ocean regions where individuals were tracked, mean monthly CRI values were highest in the northwest Indian Ocean, north Atlantic, and the east Pacific regions (Fig. 4 *A* and *B* and *SI Appendix*, Table S6). Individuals occupying the northwest Indian Ocean and the north Atlantic had the highest CRI estimates (pairwise Wilcoxon rank-sum tests; *SI Appendix*, Table S10*A*). The lowest CRI values were reported in the south Atlantic and southwest Indian Ocean regions (Fig. 4*B*). Individuals experienced the highest CRI from cargo vessels followed by tanker vessels, whereas large fishing vessels were associated with the lowest mean monthly CRI across all regions in the study (Fig. 4*C* and *SI Appendix*, Table S7; for a detailed description of regional overlap and CRI see *SI Appendix*, section 4.6). We carried out additional analyses to determine whether spatial overlap and CRI estimates were sensitive to different grid cell sizes and satellite tag spatial accuracies (*SI Appendix*, Table S11), different year sets (*SI Appendix*, Table S12), variations in actual shark depth use (*SI Appendix*, Table S13 and Fig. S11), and AIS data sources (*SI Appendix*, Table S14). However, we found no substantial effects of these variations on the patterns of spatial overlap and CRI estimates reported globally (*SI Appendix*, section 4.8).

Hotspots of mean monthly CRI (defined here as ≥90th percentile of relative CRI) were identified across all major oceans. For example, there were CRI hotspots (Fig. 4*A* and *SI Appendix*, Fig. S3*B*) in the Atlantic Ocean (Gulf of Mexico and between Haiti and Cuba), in the Indian Ocean (the Red Sea, Arabian Gulf, between western Australia and Indonesia, and the Perth Canyon area), and in the Pacific Ocean (around Baja California, Gulf of Panama, the northern coast of New Guinea, and where the northern Coral Sea meets the Solomon Sea). There were areas of high whale shark density in many coastal regions where vessel traffic density was also high, and these locations accounted for some of the highest CRI values. We found that mean global CRI calculated spatially (Fig. 4*A*) was significantly higher in coastal regions than oceanic waters (*t* test, $t = -6.79$, $n = 5{,}897$ cells, $P < 0.001$), despite greater time spent by sharks in the collision zone in oceanic locations (*SI Appendix*, Table S3). We also found that there was a 29.6% overlap between whale shark space-use hotspots (Fig. 2*A* and *SI Appendix*, Fig. S3*A*) and hotspots of potential collision risk (Fig. 4*A* and *SI Appendix*, Fig. S3*B*), confirming that extensive areas exist where the highest density areas of whale sharks co-occur with areas of highest potential collision risk with large vessels. For example, areas with active ports located around semienclosed gulfs—where land mass constrains sharks and vessels into reduced spaces, such as in the Arabian Gulf—were hotspots of both whale shark space use (Fig. 2*A* and *SI Appendix*, Fig. S3*A*) and CRI (Fig. 4*A* and *SI Appendix*, Fig. S3*B*). Mean monthly CRI in largely semienclosed waters (e.g., Gulf of Mexico, Arabian Gulf, Red Sea) were compared separately and individuals occupying the Arabian Gulf (the second-largest whale shark aggregation in the world) were exposed to significantly greater potential collision risk than those occupying the Gulf of Mexico (pairwise Wilcoxon rank-sum test; *SI Appendix*, Table S10*D* and Fig. S12) as well as the highest frequency of confirmed whale shark mortality due to large vessel collision (Fig. 4*D* and *SI Appendix*, Table S8). Globally, mean monthly CRI remained relatively constant across the year, with the lowest risk in September and October and highest from May to August and from November to February (*SI Appendix*, Fig. S4). Regionally, mean monthly CRI of individuals fluctuated, as the monthly space used by whale sharks shifted away from and back to heavily used vessel areas (Figs. 2*C* and 3 *A*–*C* and *SI Appendix*, Figs. S6 and S9). Our approach identifies when the risks of collision with large vessels are likely to be higher in overlap hotspots.

Potential Mortality Events. The results show high overlap of whale shark hotspots and traffic that predict higher risk of collisions, and CRI correlates positively with regional frequency of fatal collisions. However, while our approach cannot provide direct evidence of lethal ship strikes of tracked sharks, dive profiles and the last known satellite-transmitted locations of marine megafauna are a potentially valuable tool to infer mortality events (31). Depth data obtained from pop-off satellite archival transmitter (PSAT) tags were analyzed to determine if animal vertical movements were consistent with normal behaviors or instead showed characteristics of mortality events, such as slow sinking to the seafloor in the case of negatively buoyant whale sharks (*SI Appendix*, section 4.1.1). One individual we tracked in the Gulf of Mexico had a final dive profile consistent with mortality based on the rate of the final vertical descent which was unusually slow (4.46 $m \cdot min^{-1}$ ± 0.89 SD) compared to other deep dives occurring prior to this event (dives with a maximum depth >1,000 m: 36.46 $m \cdot min^{-1}$ ± 25.58 SD) (Fig. 5*A*). The tag popped off and floated to the surface on reaching the maximum depth limit of the device, indicating a probable mortality and subsequent sinking event. Interestingly, this event occurred in an area with 97.4 vessels per ∼784 km^2 (within the 1° × 1° resolution cell where the track ended, which is more than three times greater than areas considered busy; 31 vessels 2011 to 2014 annual mean; Fig. 5*A*). Final dive profiles of a further six tracked whale sharks where maximum tag-depth limits were exceeded were recorded, suggesting additional lethal ship strikes may have occurred (*SI Appendix*, Fig. S13). To examine this possibility further we analyzed the final locations of all tracked whale sharks in relation to vessel densities. While transmitters can fail and cease transmitting for a number of reasons unrelated to mortality (32, 33), we reasoned that normal technical failure or loss of satellite transmitters would 1) occur randomly along a shark's trajectory rather than 2) being more frequently associated with areas of higher vessel activity. We tested both these possibilities (see *Methods*) and found that the overlap of actual last locations of sharks

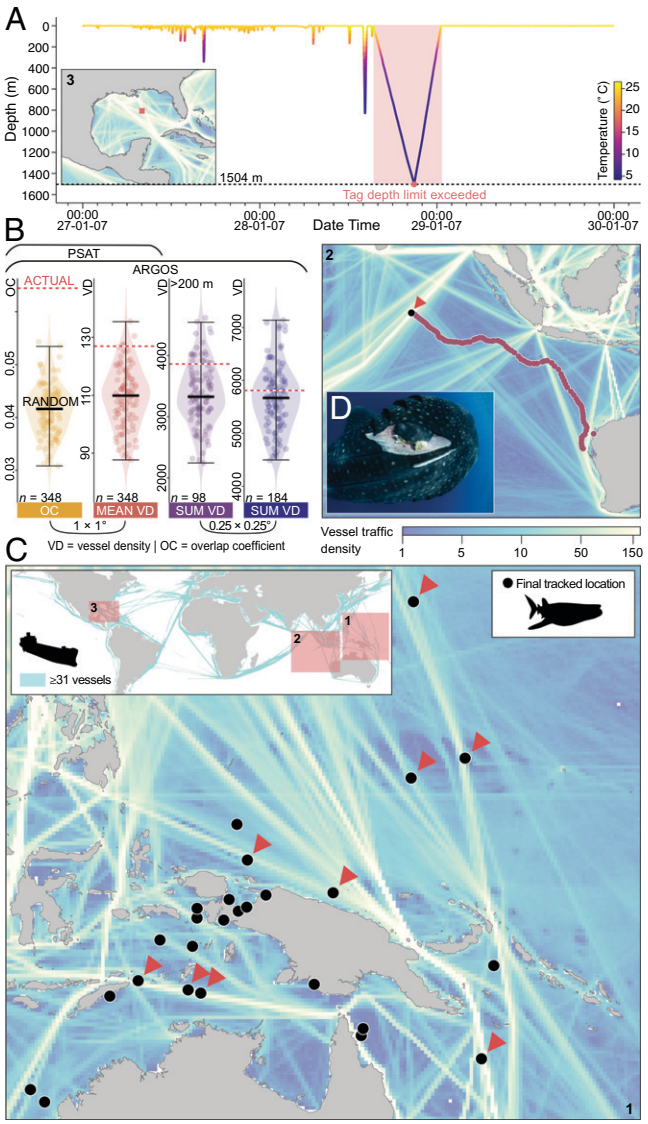

Fig. 5. Final tracked locations in relation to vessel traffic. (*A*) Time series depth profile of an individual shark showing depth use toward the end of the tracking period. Normal diving behavior was apparent before the red highlighted segment where an unusually slow descent (4.46 m·min^{-1} ± 0.89 SD) occurred until a depth of 1,504 m (black dotted line), when the tag was released and floated to the surface. This type of observation occurs as a result of an individual dying and slowly sinking. (*Inset*) Tag pop-off location within a heavily trafficked area in the central Gulf of Mexico where the average density within the 1° × 1° cell where the track ended was 97.42 vessels per ~784 km^2 (2011 to 2014 annual mean). (*B*) Differences between the actual final locations and randomized runs of final locations (n = 100) for the overlap coefficient (*Far Left*; OC, $P < 0.001$, 95% CI: [0.041, 0.042]) and mean vessel density (*Center*; VD, $P < 0.001$, 95% CI: [107.16, 111.25]) for all tracks (n = 348) at the 1° × 1° cell resolution scale. (*Far Right*) The sum of VD within cells for all ARGOS locations (n = 184, $P < 0.05$, 95% CI: [5,548.89, 5,792.73]). (*Center Right*) The oceanic ARGOS locations only (>200-m depth; n = 98, $P < 0.001$, 95% CI: [3,292.11, 3,523.76]) at the 0.25° × 0.25° cell resolution scale. Violin plots and points show spread of the randomized data (n = 100), thick lines show the median of randomized runs, and the dotted red line shows the actual final location values. Points have been spread for ease of interpretation. (*C*) Global binary map of busy shipping routes (defined as the 90th percentile of vessel density within a cell; 31 for the 2011 to 2014 annual mean). Highlighted regions show (1) fine-scale examples of final tracked locations and vessel traffic density (2011 to 2014 annual mean) in the west Pacific region, where red arrows highlight examples of final locations overlapping with or close to busy shipping routes and (2) an example of an individual whale shark in the east Indian Ocean region where it travels offshore from the tagging site at Ningaloo, Australia (tracking duration, 92 d; distance traveled, 4,971.78 km) and ceases transmission while in a busy shipping route (vessel density, 375.25). (*D*) Example of a collision outcome in the form of a major-vessel-related injury on the dorsal surface of a whale shark; credit: S.J.P.

within busiest routes (characterized as ≥90th percentile of unique vessel counts within grid cells; 31 vessels for the 2011 to 2014 annual mean) was greater than for randomly selected potential "last" locations (n = 348 locations; overlap coefficient, OC = 0.065, $P < 0.001$, 95% CI: [0.041, 0.042]) (Fig. 5*B*). In addition, the mean vessel traffic density at actual last locations of sharks was significantly greater than expected compared to random (n = 348 locations, mean = 126.93 vessels, $P < 0.001$, 95% CI: [107.16, 111.25]) at the 1° × 1° cell resolution scale. Repeating this using only ARGOS transmitter tracked sharks (n = 256 tracks) that are more spatially accurate than PSAT tags, showed the same results ($t = -2.28$, n = 184 locations, sum = 5,810.92, $P < 0.05$, 95% CI: [5,548.89, 5,792.73]) as well as for those located in oceanic waters (>200 m depth, $t = -7.78$, n = 98 locations, sum = 3,862, $P < 0.001$, 95% CI: [3,292.11, 3,523.76]) at the 0.25° × 0.25° cell resolution scale (Fig. 5*B*). For ARGOS tags where we had transmitted diagnostic information available (n = 62 tracks), we found nine instances of potential technology-related failure which were linked to either battery exhaustion (n = 2 tracks, 3.23%) or bio-fouling (n = 7 tracks, 11.29%), indicating a probable failure rate of 14.5% of tags (total recorded technical failures = 14.52%; *SI Appendix*, Fig. S14). However, this was not the case for any of the tracks where observed final transmitted locations occurred in the most heavily used vessel areas (n = 8 tracks). Overall, we found that 28% of ARGOS tracks (61 of 219 tracks) that were not classed as too close to land ended in the busiest vessel areas (Fig. 5*C*). By extrapolation, we estimate that 14.5% of tags that ended on a busy route were also the result of technical failure, leaving 85.5% of tracks that ended for other reasons. Consequently, it is possible that 85.5% of the 61 tracked tags that ceased transmitting on busy routes (52 tracks, or 23.7% of all 219 ARGOS tracks) did so for reasons unrelated to random technical failure. We propose that lethal ship strikes may have been responsible for a substantial proportion of these but were undetected or unreported by vessels.

Conclusions

Our results provide global estimates of the potential collision risk posed by burgeoning large-vessel marine traffic to an ocean giant. We found whale shark horizontal space use overlap with large, AIS-tracked vessels was spatially and temporally extensive across their entire range including many important aggregation areas (*SI Appendix*, Tables S15 and S16), and CRI correlated with reported regional collision mortalities of whale sharks, suggesting potential widespread effects on populations. Continuing population declines in the majority of areas where whale sharks are known to aggregate remain unclear (*SI Appendix*, Table S16) (15), and there is currently no mandated monitoring or formalized assessment to determine the impacts of large vessel collisions. Thus, we suggest that the risk posed to whale sharks is likely greater than currently realized and may represent a substantial source of "cryptic" mortality that remains unquantified for this endangered species and that, without mitigation, may lead to further population decline.

Development of collision-focused mitigation is vital because whale sharks are subjected to additional human-related threats (16, 34) that when acting simultaneously alongside the potentially high instances of large-vessel-induced mortality identified here may exacerbate declines and inhibit long-term survivorship. In addition, persistent large-vessel activity in areas used by whale sharks may have complex, sublethal impacts on essential aspects of the species' behavior and physiology. Mitigation for other at-risk megafauna is already in place in some whale shark CRI hotspots identified here, and real-time whale-vessel

monitoring initiatives have been developed to help reduce collisions (e.g., https://www.whalesafe.com and https://www.whalealert.org) (35, 36). However, to our knowledge, many areas occupied by whale sharks remain unprotected by these measures (*SI Appendix*, section 4.10). As a first step to address this problem, an international reporting scheme aiming to consolidate collision records is needed to ensure visibility and support regional implementation of management measures. Second, mitigation measures such as separating vessels from individuals and reducing vessel speeds appear necessary in some of the high-risk areas we identified (*SI Appendix*, section 4.10). For example, in areas where aggregations form in dense traffic such as the southern Red Sea and Arabian Gulf, and where sharks seasonally transit shipping lanes, such as northward and southward shark movements off western Australia (*SI Appendix*, Fig. S7), reductions in vessel speed could be mandated at a national or international level to reduce the potential for lethal collisions. For large whale populations, the probability of lethal injuries resulting from collisions decreased to <50% when vessels traveled at speeds ≤10 kn (~5 $m \cdot s^{-1}$) (29). This relationship is yet to be determined for whale sharks; however, we report vessel speeds at the closest point of approach that often exceeded this threshold (*SI Appendix*, Table S4*B*). It is crucial to explore this relationship further if we are to advance toward effective and sustainable speed-mitigation strategies for whale sharks. In addition to reducing the likelihood of lethal collisions (29), reductions in speed can also have wider benefits including quieter and cleaner oceans (37). Reductions across the entire global shipping fleet by as little as 10% could reduce overall greenhouse gas emissions by around 13%, improving the likelihood of the IMO meeting emissions targets for 2050 and reducing the total sound energy from shipping by around 40% (37).

The substantial hidden mortality we propose for whale sharks may also be occurring for other marine megafauna. Our approach based on worldwide tracking of animal movements and vessels could be adopted to estimate range-wide vessel collision risks with other threatened or endangered surface-dwelling species, especially those that are less-well-studied globally than whale sharks, such as other fish (e.g., basking shark, *Cetorhinus maximus*; ocean sunfish, *Mola* spp.), sea turtles (e.g., leatherback, *Dermochelys coriacea*), and baleen whales (e.g., Indian Ocean blue whales, *Balaenoptera musculus*), where global collaboration could provide the opportunity to explore large datasets. Estimating risk throughout a species' distributional range provides a means to identify areas of greatest potential threat and where mitigation measures could be best focused.

Methods

Shark Tracking. A total of 348 whale sharks were tagged with satellite-linked transmitters between 2005 and 2019 in the Atlantic, Indian, and Pacific Oceans. Fine-scale shark movements were monitored with FastLoc GPS tags in the Gulf of Mexico. Vertical space use was assessed from swimming depth data recorded by pressure-sensitive pop-off satellite-linked archival transmitter tags. Each daily location estimate of an individual was weighted by the inverse of the number of all individuals with location estimates for the same relative day of their track. Weights for all locations were normalized so that they summed to unity to ensure all individuals contributed equally to global whale shark relative-spatial-density estimates. Details are given in *SI Appendix*, section 1.

Vessel Tracking. We used AIS data to assess marine traffic patterns. Gridded products were purchased from Exact Earth (https://www.exactearth.com) for the years of 2011 to 2014 at 0.25° × 0.25° grid cell resolution, coverage that matched the majority of shark tracking data. To check that the main AIS dataset was representative of AIS vessel movement patterns from different data providers, we also analyzed data for 2014 and 2017 to 2019 provided by Global Fishing Watch (https://globalfishingwatch.org). Fine-scale vessel movement data in the Gulf of Mexico were from the National Oceanic and Atmospheric Administration (https://coast.noaa.gov). Details are given in *SI Appendix*, section 1.

Spatial Overlap. Spatial overlap was calculated as the number of 0.25° × 0.25° grid cells where both whale sharks and vessels were located, as a function of all whale shark grid cells occupied in a mean month. Details are given in *SI Appendix*, section 1.

CRI. A potential collision exposure index was defined as the number of vessels that a whale shark may be exposed to in the same relative month and grid cell and was calculated as the product of vessel traffic density and collision zone use (shark depth use). CRI was calculated as the product of shark spatial density and potential collision exposure index and pertains to an individual shark per month. The relationship between estimated CRI and confirmed vessel-induced mortality was assessed with a collision mortality database for whale sharks dating back to 1930 compiled from literature and online searches and communications with experts. Details are given in *SI Appendix*, section 1.

Data Availability. The derived mean shark relative spatial density and data underlying Fig. 4*A* (map of mean shark–vessel spatial overlap and CRI) and Fig. 4*B* (plot of spatial overlap and CRI) is freely available on GitHub (https://github.com/GlobalSharkMovement/GlobalCollisionRisk) (38).

ACKNOWLEDGMENTS. Funding for data analysis was provided by the UK Natural Environment Research Council (NERC) through a University of Southampton INSPIRE DTP PhD Studentship to F.C.W. Additional funding for data analysis was provided by NERC Discovery Science (NE/R00997/X/1) and the European Research Council (ERC-AdG-2019 883583 OCEAN DEOXYFISH) to D.W.S., Fundação para a Ciência e a Tecnologia (FCT) under PTDC/BIA/28855/2017 and COMPETE POCI-01–0145-FEDER-028855, and MARINFO–NORTE-01–0145-FEDER-000031 (funded by Norte Portugal Regional Operational Program [NORTE2020] under the PORTUGAL 2020 Partnership Agreement, through the European Regional Development Fund–ERDF) to N.Q. FCT also supported N.Q. (CEECIND/02857/2018) and M.V. (PTDC/BIA-COM/28855/2017). D.W.S. was supported by a Marine Biological Association Senior Research Fellowship. All tagging procedures were approved by institutional ethical review bodies and complied with all relevant ethical regulations in the jurisdictions in which they were performed. Details for individual research teams are given in *SI Appendix*, section 8. Full acknowledgments for tagging and field research are given in *SI Appendix*, section 7. This research is part of the Global Shark Movement Project (https://www.globalsharkmovement.org).

Author affiliations: [a]Marine Biological Association of the United Kingdom, Plymouth PL1 2PB, United Kingdom; [b]Ocean and Earth Science, National Oceanography Centre Southampton, University of Southampton, Southampton SO14 3ZH, United Kingdom; [c]CIBIO, Centro de Investigação em Biodiversidade e Recursos Genéticos, InBIO Laboratorio Associado/BIOPOLIS Program in Genomics, Biodiversity and Land Planning, Universidade do Porto, 4485-668 Vairão, Portugal; [d]Mote Marine Laboratory, Sarasota, FL 34236; [e]College of Science and Engineering, James Cook University, Cairns, QLD 4878, Australia; [f]Biopixel Oceans Foundation, Cairns, QLD 4878, Australia; [g]Marine Data Technology Hub, James Cook University, Cairns, QLD 4870, Australia; [h]Large Marine Vertebrates Research Institute Philippines, Bohol 6308, Philippines; [i]Marine Research and Conservation Foundation, Lydeard St Lawrence TA4 3SJ, United Kingdom; [j]Qatar Whale Shark Research Project, Doha, Qatar; [k]Red Sea Research Center, Division of Biological and Environmental Science and Engineering, King Abdullah University of Science and Technology, Thuwal 23955, Kingdom of Saudi Arabia; [l]Fundación Malpelo y Otros Ecosistemas Marinos, Bogata 110111, Colombia; [m]School of Aquatic and Fishery Sciences, University of Washington, Seattle, WA 98105; [n]Biology Department, Woods Hole Oceanographic Institution, Woods Hole, MA 02543; [o]St Helena Government, Jamestown STHL 1ZZ, St Helena; [p]Ch'ooj Ajuail AC, 77509 Cancún, Mexico; [q]Madagascar Whale Shark Project, Nosy Be, Madagascar; [r]Georgia Aquarium, Atlanta, GA 30313; [s]School of Biomedical Sciences, The University of Queensland, St. Lucia, QLD 4072, Australia; [t]Conservation International New Zealand, University of Auckland, Auckland 1010, New Zealand; [u]Dirección Parque Nacional Galapagos, Puerto Ayora, Galapagos Islands, Ecuador; [v]MigraMar, Olema, CA 94956; [w]Comisión Nacional de Áreas Naturales Protegidas, Cancún 77500, México; [x]Galapagos Whale Shark Project, Puerto Ayora, Galapagos Islands, Ecuador; [y]Smithsonian Tropical Research Institute, Panama 0843-03092, Republic of Panama; [z]Conservation International Raja Ampat, West Papua 98416, Indonesia; [aa]Departamento de Pesca e Aquicultura, Universidade Federal Rural de Pernambuco, Recife/PE 52171-900, Brazil; [bb]Galapagos Science Center, Universidad San Francisco de Quito, Quito 170901, Ecuador; [cc]OCEARCH, Park City, UT 84068; [dd]Qatar Ministry of Municipality and Environment, Doha, Qatar; [ee]Okeanos R&D Centre, University of the Azores, 9900-140 Horta, Portugal; [ff]Harry Butler Institute, Murdoch University, Murdoch, WA 6150, Australia; [gg]ECOCEAN Inc., Serpentine, WA 6125, Australia; [hh]Marine Megafauna Foundation, Truckee, CA 96161; [ii]Whale Shark

Mexico, Conexiones Terramar AC, 23205 La Paz, Mexico; [jj]School of Biological Sciences, The University of Queensland, St Lucia, QLD 4072, Australia; [kk]Oceans and Atmosphere, Commonwealth Scientific and Industrial Research Organisation, St Lucia, QLD 4067, Australia; [ll]Centre for Applications in Natural Resource Mathematics, School of Mathematics and Physics, The University of Queensland, St Lucia, QLD 4067, Australia; [mm]Sundive Research, Byron Bay, NSW 2481, Australia; [nn]Marine Conservation Society Seychelles, Mahe, Seychelles; [oo]Department of Biological Sciences, The Guy Harvey Research Institute, Nova Southeastern University, Dania Beach, FL 33004; [pp]Conservation International Indonesia, Jakarta 12550, Indonesia; [qq]Massachusetts Division of Marine Fisheries, New Bedford, MA 02744; [rr]Department of Biological Science, University of Rhode Island, Kingston, RI 02881; [ss]Global Fishing Watch, Washington, DC, 20036; [tt]Australian Institute of Marine Science, Indian Ocean Marine Research Centre, University of Western Australia, Crawley, WA 6009, Australia; [uu]Oceans Graduate School and Oceans Institute, The University of Western Australia, Crawley, WA 6009, Australia; [vv]Oceans Institute and School of Biological Sciences, The University of Western Australia, Crawley, WA 6009, Australia; [ww]Instituto de Fisica Interdisciplinar y Sistemas Complejos, Consejo Superior de Investigaciones Cientificas-University of the Balearic Islands, E-07122 Palma de Mallorca, Spain; and [xx]Centre for Biological Sciences, University of Southampton, Southampton SO17 1BJ, United Kingdom

Author contributions: F.C.W. and D.W.S. designed research; F.C.W., N.E.H., N.Q., J.P.T., K.A., G.A., S.S.B., A.B., M.L.B., S.B.L., C.D.B., E.C., J.E.M.C., R.d.l.P., S.D., A.D.M.D., C.L.D., M.V.E., E.E., R.F., J.G.C., J.R.G., H.M.G., R.H., A.H., F.H.V.H., A.R.H., R.E.H., M.Y.J., J.L., F.L., B.C.L.M., J.J.M.J., B.M.N., C.P.-P., S.J.P., L.M.Q., D.R.-M., S.D.R., A.J.R., D.P.R., C.A.R., D.R.L.R., M.S., M.S.S., A.B.S., G.B.S., G.S., I.S., S.R.T., D.H.W., B.M.W., D.A.K., M.T., L.C.F., M.G.M., L.M.A., E.K.L., M.M.M., L.R.P., A.M.M.S., and D.W.S. performed research; F.C.W., N.E.H., N.Q., M.V., I.d.C, M.F., T.D.W., T.C., V.M.E., and C.M.D. contributed new reagents/analytic tools; F.C.W., N.E.H., N.Q., M.V., I.d.C., J.P.T., and D.W.S. analyzed data; and F.C.W., N.E.H., and D.W.S. wrote the paper.

1. United Nations Conference on Trade and Development (UNCTAD), Review of maritime transport 2020 (2020). https://unctad.org/system/files/official-document/rmt2020_en.pdf. Accessed 25 January 2022.
2. United Nations Conference on Trade and Development (UNCTAD), Review of maritime transport 1995 (1995). https://unctad.org/system/files/official-document/rmt1995_en.pdf. Accessed 25 January 2022.
3. A. M. M. Sequeira *et al.*, Overhauling ocean spatial planning to improve marine megafauna conservation. *Front. Mar. Sci.* **6**, 639 (2019).
4. R. P. Schoeman, C. Patterson-Abrolat, S. Plön, A global review of vessel collisions with marine animals. *Front. Mar. Sci.* **7**, 292 (2020).
5. N. Queiroz *et al.*, Global spatial risk assessment of sharks under the footprint of fisheries. *Nature* **572**, 461–466 (2019).
6. B. Worm *et al.*, Global catches, exploitation rates, and rebuilding options for sharks. *Mar. Policy* **40**, 194–204 (2013).
7. D. W. Laist, A. R. Knowlton, J. G. Mead, A. S. Collet, M. Podesta, Collisions between ships and whales. *Mar. Mamm. Sci.* **17**, 35–75 (2001).
8. C. M. Duarte *et al.*, The soundscape of the Anthropocene ocean. *Science* **371**, eaba4658 (2021).
9. M. Stelfox, J. Hudgins, M. Sweet, A review of ghost gear entanglement amongst marine mammals, reptiles and elasmobranchs. *Mar. Pollut. Bull.* **111**, 6–17 (2016).
10. E. W. Gudger, Whale sharks rammed by ocean vessels: How these sluggish leviathans aid in their own destruction. *N. Engl. Nat.* **7**, 1–10 (1940).
11. S. D. Kraus *et al.*, Ecology. North Atlantic right whales in crisis. *Science* **309**, 561–562 (2005).
12. International Whaling Commission, "Annual Report of the International Whaling Commission 2005" (International Whaling Commission, 2005).
13. M. Meekan *et al.*, Asymptotic growth of whale sharks suggests sex-specific life-history strategies. *Front. Mar. Sci.* **7**, 774 (2020).
14. D. Rowat, K. S. Brooks, A review of the biology, fisheries and conservation of the whale shark Rhincodon typus. *J. Fish Biol.* **80**, 1019–1056 (2012).
15. S. J. Pierce, B. Norman, Whale shark (Rhincodon typus). The IUCN Red List of Threatened Species 2016. https://dx.doi.org/10.2305/IUCN.UK.2016-1.RLTS.T19488A2365291.en. Accessed 25 January 2022.
16. D. Rowat, F. C. Womersley, B. M. Norman, S. J. Pierce, "Global threats to whale sharks" in *Whale Shark Biology, Ecology, and Conservation*, A. D. M. Dove, S. J. Pierce, Eds. (CRC Press, 2021), chap. 11, pp. 239–265.
17. F. Womersley, J. Hancock, C. T. Perry, D. Rowat, Wound-healing capabilities of whale sharks (Rhincodon typus) and implications for conservation management. *Conserv. Physiol.* **9**, a120 (2021).
18. A. M. M. Sequeira, C. Mellin, D. A. Fordham, M. G. Meekan, C. J. Bradshaw, Predicting current and future global distributions of whale sharks. *Glob. Change Biol.* **20**, 778–789 (2014).
19. D. P. Robinson *et al.*, Some like it hot: Repeat migration and residency of whale sharks within an extreme natural environment. *PLoS One* **12**, e0185360 (2017).
20. A. H. Cordesman, *Iran, Oil, and the Strait of Hormuz* (Center for Strategic and International Studies, Washington, DC, 2007)
21. A. M. M. Sequeira, C. Mellin, M. G. Meekan, D. W. Sims, C. J. Bradshaw, Inferred global connectivity of whale shark Rhincodon typus populations. *J. Fish Biol.* **82**, 367–389 (2013).
22. H. Blondin, B. Abrahms, L. B. Crowder, E. L. Hazen, Combining high temporal resolution whale distribution and vessel tracking data improves estimates of ship strike risk. *Biol. Conserv.* **250**, 108757 (2020).
23. D. A. Kroodsma *et al.*, Tracking the global footprint of fisheries. *Science* **359**, 904–908 (2018).
24. G. K. Silber, J. Slutsky, S. Bettridge, Hydrodynamics of a ship/whale collision. *J. Exp. Mar. Biol. Ecol.* **391**, 10–19 (2010).
25. S. J. Pierce, A. Méndez-Jiménez, K. Collins, M. Rosero-Caicedo, A. Monadjem, Developing a Code of Conduct for whale shark interactions in Mozambique. *Aquat. Conserv.* **20**, 782–788 (2010).
26. P. J. Haskell *et al.*, Monitoring the effects of tourism on whale shark Rhincodon typus behaviour in Mozambique. *Oryx* **49**, 492–499 (2014).
27. L. Chapuis *et al.*, The effect of underwater sounds on shark behaviour. *Sci. Rep.* **9**, 6924 (2019).
28. D. P. Nowacek, M. P. Johnson, P. L. Tyack, North Atlantic right whales (Eubalaena glacialis) ignore ships but respond to alerting stimuli. *Proc. Biol. Sci.* **271**, 227–231 (2004).
29. A. S. Vanderlaan, C. T. Taggart, Vessel collisions with whales: The probability of lethal injury based on vessel speed. *Mar. Mamm. Sci.* **23**, 144–156 (2007).
30. A. L. Quiros, Tourist compliance to a Code of Conduct and the resulting effects on whale shark (Rhincodon typus) behavior in Donsol, Philippines. *Fish. Res.* **84**, 102–108 (2007).
31. G. C. Hays, Tracking animals to their death. *J. Anim. Ecol.* **83**, 5–6 (2014).
32. G. C. Hays, C. J. A. Bradshaw, M. C. James, P. Lovell, D. W. Sims, Why do Argos satellite tags deployed on marine animals stop transmitting? *J. Exp. Mar. Biol. Ecol.* **349**, 52–60 (2007).
33. G. C. Hays, J. O. Laloë, A. Rattray, N. Esteban, Why do Argos satellite tags stop relaying data? *Ecol. Evol.* **11**, 7093–7101 (2021).
34. S. D. Reynolds *et al.*, Regional variation in anthropogenic threats to Indian Ocean whale sharks. *Glob. Ecol. Conserv.* **33**, e01961 (2022).
35. B. Abrahms *et al.*, Dynamic ensemble models to predict distributions and anthropogenic risk exposure for highly mobile species. *Divers. Distrib.* **25**, 1182–1193 (2019).
36. M. F. Baumgartner *et al.*, Persistent near real-time passive acoustic monitoring for baleen whales from a moored buoy: System description and evaluation. *Methods Ecol. Evol.* **10**, 1476–1489 (2019).
37. R. Leaper, The role of slower vessel speeds in reducing greenhouse gas emissions, underwater noise and collision risk to whales. *Front. Mar. Sci.* **6**, 505 (2019).
38. F. C. Womersley *et al.*, GlobalSharkMovement/GlobalCollisionRisk. GitHub. https://github.com/GlobalSharkMovement/GlobalCollisionRisk. Deposited 9 March 2022.